

The Bioactivity of Green-Synthesized Noble Metal Nanoparticles Against Streptomycin-Resistant *Bacillus* Sp. Is Enhanced by Bioconjugation with Streptomycin

[N. Ramasami](#)^{*}, [M. Dhayan](#)^{*}, M. Selvaraj, [S. U. Mohammed Riyaz](#), Perumal Palani, Raja kumar Kanthapazham, [D. Zhrebtsov](#), [J. C. Mejuto](#), [J. Simal-Gandara](#)^{*}, [A. Cid-Samamed](#)^{*}

Posted Date: 17 February 2023

doi: 10.20944/preprints202302.0291.v1

Keywords: *Garcinia mangostana* L.; Rind Extract; Antibiotic-Resistant; Streptomycin; Bioconjugation; Hemocompatibility



Preprints.org is a free multidiscipline platform providing preprint service that is dedicated to making early versions of research outputs permanently available and citable. Preprints posted at Preprints.org appear in Web of Science, Crossref, Google Scholar, Scilit, Europe PMC.

Copyright: This is an open access article distributed under the Creative Commons Attribution License which permits unrestricted use, distribution, and reproduction in any medium, provided the original work is properly cited.

Article

The Bioactivity of Green-Synthesized Noble Metal Nanoparticles Against Streptomycin-Resistant *Bacillus Sp.* Is Enhanced by Bioconjugation with Streptomycin

N. Ramasami ^{1,*}, M. Dhayalan ^{2,3,*}, M. Selvaraj ⁴, S. U. Mohammed Riyaz ⁵, P. Palani ⁴, Raja kumar K. ⁶, D. Zherebtsov ⁶, J. C. Mejuto ⁹, J. Simal- Gandara ^{7,8,*} and A. Cid-Samamed ^{9,*}

¹ Depart. of Biotechnology, College of Science and Humanities, SRMIST, Kattankulathur – 603203, TamilNadu, India.

² Division of Formulation and Development of Small Molecules and Drug Discovery Group, Anticancer Bioscience, Tianfu International Biotown Chengdu, 610000 China.

³ Depart. of Prosthodontics, Saveetha Dental College & Hospitals, Saveetha Institute of Medical and Technical Sciences (Saveetha University) Chennai - 600 077, TamilNadu, India

⁴ Depart. of Biotechnology, Sri Sankara Arts and Science College, Enathur, Kanchipuram, India.

⁵ PG & Research Department of Biotechnology Islamiah College (Autonomous), Vaniyambadi - 635752, Tamil Nadu, India.

⁶ Nanotechnology Research and Education Centre, South Ural State University, Chelyabinsk, 454080, Russia.

⁷ CISPAC, Fontan Building, City of Culture, E15707 Santiago de Compostela; <https://cispac.gal/>

⁸ Universidade de Vigo, Nutrition and Bromatology Group, Analytical Chemistry and Food Science Department, Faculty of Science, E32004, Ourense, Spain

⁹ Physical Chemistry Department, Faculty of Sciences, University of Vigo, E-32004 Ourense, Spain.

* Correspondence: shared between N. Ramasami, M. Dhayalan, A. Cid-Samamed, and Prof. J. Simal Gandara: nishantr@srmist.edu.in* manikandandhayalan88@gmail.com* jsimal@uvigo.es* acids@uvigo.es*

Abstract: Background: Combinatorial therapy- “nano antibiotics” is an emerging field in nanoscience. In this present investigation, we attempted to combine the green synthesized noble metal nanoparticle and the antibiotic Streptomycin to form bio-conjugated nanoparticles. The newly synthesized Nano antibiotics acted as the antibiotic carrier, functioned as cargo, and delivered the antibiotic. Methods: Comparative studies between the noble metal nanoparticles were attempted for the first time on the grounds of their antibacterial activity. The antibacterial activity of the three noble metal nanoparticles was assessed against Streptomycin-resistant *Bacillus sp.*; the results obtained proved that silver nanoparticles were a potent antibacterial agent. Still, no antibacterial activity was exerted by gold, and platinum nanoparticles were for the Streptomycin-resistant strain *Bacillus sp.* To our surprise, the gold and platinum fabricated/bio-conjugated nanoparticle with the antibiotic showed 100% antibacterial activity, whose antibacterial activity was zero when functioning as a nanoparticle alone. Results: The combinatorial therapy of two different clauses of drugs majorly increased antibacterial activity. It enhanced the antibiotic to overcome the resistance exhibited by the bacterial pathogen, and the possible mechanism is elucidated in the present study. Also, an attempt has been made to assess the nanotoxicity of the nano-bioconjugates on RBC and compare their hemocompatibility. The results obtained in the current investigation demonstrate the enhanced antibacterial activity of the green synthesized nanoparticles conjugated with the streptomycin; their efficacy for combinational therapy against resistance in pathogenic organisms highlights the novelty of the work and the comparative study of three different noble metals nanoparticles (Ag, Au, Pt) from single agro-waste for the first time.

Keywords: *Garcinia mangostana* L.; Rind Extract; Antibiotic-Resistant; Streptomycin; Bioconjugation; Hemocompatibility

1. Introduction

Neu [1] proposed that the need for new antibiotics would have to continue as bacteria can overcome each new antimicrobial agent discovered. There are evident reports on the constant increase in antimicrobial resistance against all major classes of antibiotics, which are in treatment against a wide variety of diseases [2]. In general, two major antibiotics classes are aminoglycosides and glycopeptides. These are clinically important as they are the last line of defense against resistant bacteria that develop resistance to antibiotics such as penicillin, methicillin, and other β lactams [3]. Neu and Gootz [4] have suggested that the bacteria contain some enzymes in their periplasmic space, which catalyze the addition of acetyl, phosphoryl, and adenylyl ions of aminoglycoside to various degrees [5]. The modified aminoglycoside antibiotic fails to bind to the ribosome leading to poor antibiotic uptake by bacteria and the development of antibiotic resistance towards the antibiotic. The resistance developed by bacteria can be overcome by employing combinatorial therapy. Using two or more drugs to prevent the emergence of resistance could be effective; however, using drug combinations to achieve synergy has been seen as more complicated. It has been highlighted that some of the best combinations in the form of anti-cell wall agents with an aminoglycoside, which act on different metabolic steps in the bacterial metabolic or synthetic pathway, and the use of β -lactamase inhibitors with β -lactamase susceptible antibiotics have been suggested.

Nanomedicine and nanotoxicity are considered the two sides of the same coin, and the minimization of nanotoxicity is a crucial concern given the potential application of nanoparticles in nanomedicine, especially when administered through systemic circulation [6]. Red blood cells (biconcave discoid cells filled with hemoglobin and lacking organelles, including the nucleus) represent the most abundant cellular constituent of the blood (>99%) and play an essential role in drug delivery. Drug delivery systems circulating in the blood often encounter RBCs, which may lead to unintended effects of the drug on RBCs, and *vice versa*. The interaction of drug delivery systems (e.g., polymeric nanocarriers) with RBCs and their consequences are highly significant in mechanistic and translational aspects [7].

Blood, directly or indirectly, encounters the hazardous nanoparticles and transports the foreign substances into the cells, tissues, and organs. Therefore, it is imperative to study the nanotoxicity exerted by nanoparticles on blood, particularly on the erythrocytes. More importantly, many biomedical applications of nanoparticles require direct injection into the body through different routes of administration, which leads to direct contact of the nanoparticles with blood components. Li Qiang [8,9] have suggested that the evaluation of the compatibility of metal nanoparticles with blood is necessary and much importance has to be given to studying the interaction of nanoparticles with blood components.

Therefore, it has been hypothesized in the present investigation that the resistance shown by *Bacillus* sp. to streptomycin could be due to the poor uptake by the bacterium. The poor uptake can be overcome by incorporating the antibiotic with the anti-cell wall agent, presumably making pores in the bacterial cell wall and enabling the agent to penetrate the cell. Metal nanoparticles [10] are the best antimicrobial agent as they are supposed to cause damage to the cell wall [11]. Therefore, an effort has been made in the present investigation to combine the green synthesized noble metal nanoparticles (Ag, Au, and Pt) with the commercial antibiotic streptomycin and evaluate their synergistic antibacterial activity against the streptomycin-resistant *Bacillus* sp. and their biocompatibility on human erythrocytes. The results obtained have been presented in this work and discussed with up-to-date literature on synergistic antimicrobial activity [12–17].

2. Materials and Methods

2.1. Materials

The metal precursors silver nitrate (AgNO_3), chloroauric acid (HAuCl_4), and hexachloroplatinic (IV) acid ($\text{H}_2\text{PtCl}_6 \cdot 6\text{H}_2\text{O}$) used in this study research were procured from Sigma Aldrich (USA). All the solutions (1mM) were prepared in sterile double distilled water.

2.2. Preparation of rind extract of *Garcinia mangostana* (GMRE)

The fruit *G. mangostana* was procured from the local market. The rind portion of the fruit was separated, washed thoroughly to remove the impurities, and air-dried at room temperature for ten days. The dried rinds were ground in a blender, and grinding was repeated thrice to obtain a fine texture and sieved through a mesh to get particles of uniform size. From this, 1.5 g was suspended in 50 ml of sterilized glass distilled water at 50°C - 70°C for 15 min. The resultant extract was filtered through Whatman No.1 filter paper, and the filtrate was stored at 4°C for further use.

2.3. Synthesis of metal nanoparticles

Freshly prepared rind extract was added to the aqueous solution of 1mM metal precursor at different ratios to obtain the nanoparticles; a 1:3 ratio of rind extract was added to AgNO₃ for the synthesis of silver nanoparticles, 1:2 ratio of rind extract was added to HAuCl₄ to form gold nanoparticles, and 1:4 ratio of rind extract was added to H₂PtCl₆ to synthesize platinum nanoparticles. Gold nanoparticles formed faster than silver and platinum nanoparticles under ambient conditions [18].

2.4. Conjugation of streptomycin with green synthesized metal nanoparticles

Conjugation of streptomycin with green synthesized metal nanoparticles was carried out by following the method of Chakraborty et al. and Mohammed Fayaz et al. [19,20] with slight modification. Briefly, 10 mg of streptomycin was mixed with 2 ml of the metal nanoparticles. The mixture was sonicated for 10 minutes in the dark and incubated overnight under shaking (108 rpm). The mixture was centrifuged, and the pellet was subjected to UV-VIS and FT-IR spectroscopic analyses to verify the conjugation of antibiotics with the metal nanoparticles. The metal nanoparticles conjugated with the antibiotics were used for testing for antibacterial activity.

2.5. Evaluation of the antibacterial activity of bare and antibiotic-conjugated nanoparticles

The disk diffusion method was used to evaluate the antibacterial activity of the bare metal nanoparticles and bio-conjugated metal nanoparticles against the streptomycin-resistant *Bacillus* sp. on Muller Hilton agar. The streptomycin-resistant *Bacillus* sp. was grown overnight in Luria Bertani Broth under shaking conditions (200 rpm) at 35°C. The inocula were prepared by diluting the overnight culture with 0.9% NaCl to 0.5 McFarland standard and spread onto the Muller Hinton (MH) Agar medium. To assess the antibacterial activity, 20 µl of the test compounds (GMRE, streptomycin, bare metal nanoparticles (AgNP, AuNP, and PtNP), and streptomycin conjugated metal nanoparticles (SAgNP, SAuNP, and SPtNP) were loaded onto the sterile disk placed on MH agar plates. The plates were incubated at 35°C for 24-48 h. The zone of inhibition was observed and measured using a zone of inhibition measurement scale (Himedia, India).

2.6. Determination of minimal inhibitory concentration

The minimum inhibitory concentration (MIC) of the bare green synthesized metal nanoparticles and streptomycin conjugated metal nanoparticles were tested against the human pathogenic bacteria using the broth dilution method. This method facilitates testing the inhibitory activity at various concentrations. The nutrient broth was supplemented with the test compounds at different concentrations. Control experiments were maintained without any of the test compounds. The test tubes containing the cells with test compounds were incubated for 24 h at 37°C. The MIC was determined by measuring the turbidity at 600 nm in a spectrophotometer and defined as the minimum concentration that inhibited the bacteria growth.

2.7. Determination of minimal bactericidal concentration (MBC)

The MBC was determined by growing the bacteria treated with nanoparticles conjugated with antibiotics on Muller Hinton Agar plates. The plates were incubated at 37°C for 24-48h. The minimum

bactericidal concentration was determined as the concentration that caused 100% growth inhibition upon treatment with antibiotics-conjugated nanoparticles. The control plates were maintained without the addition of conjugated nanoparticles.

2.8. Analysis of live and dead cells of bacteria treated with streptomycin conjugated nanoparticles by AO/PI staining

The bacterial cells treated with metal nanoparticles and streptomycin conjugated metal nanoparticles were stained with acridine orange (AO) and propidium iodide (PI) by following the protocol of Dalai et al. (2012) with minor modification. The bacterial cell suspension (500 µl) was added with 4 µl of AO (15 µg/ml in PBS) and 4 µl of PI (50 µg/ml in PBS) and incubated at room temperature for 5 min in the dark. After centrifugation at 5000 rpm for 5 min, the cell pellet obtained was resuspended in 500 µl PBS. The experiment was conducted under dark conditions to avoid the photobleaching of dyes. The untreated cells were considered as the control. The control and treated cells were examined under a fluorescent microscope (Carl Zeiss Axioskop 2 plus Microscope, Germany).

2.9. Determination of cell viability by fluorescence-activated cell sorter

The bacterial cells treated with the test compounds at their respective MIC concentration were centrifuged at 5000 rpm for 5 min at 4°C, and the pellets obtained were washed with sterile distilled water. Five µl of PI was added to each sample and incubated for 15 min at room temperature. After incubation, cells were washed with sterile distilled water to remove excess stains and analyzed by flow cytometry (BD FACS Calibur, Canada). Cells incubated without the streptomycin conjugated nanoparticles, and bare nanoparticles served as the controls.

2.10. Effect of the bare and streptomycin conjugated metal nanoparticles on the structural integrity of Bacillus sp.

The morphological changes caused by the test compounds were visualized using scanning electron microscopic analysis. A 5 ml suspension of the treated cells was centrifuged, and the pellet of cells was fixed with 50 µl of 2.5% glutaraldehyde prepared in 1x PBS for 6 h at 37°C. The cells were washed thrice with PBS (1x) (Malathi et al., 2014). The pellet was resuspended in sterile distilled water, and a small drop of it was placed on an aluminum foil and dried at room temperature. The samples were sputter-coated with gold (Hitachi E-1010 Ion Sputter, Japan) for 60 sec and observed under the scanning electron microscope (Hitachi S3400N, Japan).

2.11. Hemolytic assay and blood aggregation studies

The hemocompatibility of the bare green synthesized metal nanoparticles (AgNP, AuNP, and PtNP) and streptomycin conjugated metal nanoparticles (SAgNP, SauNP, and SPtNP) were determined by incubating the red blood cells with the test components at different concentrations and expressed in terms of percent hemolysis. The human blood samples were collected from healthy volunteers in vials coated with ethylene diamine tetraacetic acid (EDTA). The whole blood was centrifuged at 1600 rpm for 5 min, and the plasma, buffy coat, and the cells in the top layer were discarded. The packed red blood cells (RBCs) at the bottom of the tube were washed with sterile isotonic 1x PBS (pH 7.4) four times. After washing, the packed RBCs (0.2 ml) were diluted with 4.0 ml PBS, from which 0.2 ml suspension was mixed with different concentrations of the test compounds prepared in 1x PBS (0.8 ml). The diluted suspension of RBCs was added with 0.8 ml of 1x PBS and 0.8 ml of Triton X-100, which were used as negative and positive controls, respectively. The mixture was gently vortexed and incubated at room temperature for 2 h, followed by centrifugation at 1600 rpm for 5 min. The resulting supernatant was collected, and the absorbance was read at 540 nm in a UV-VIS spectrophotometer. The hemocompatibility of metal nanoparticles with or without streptomycin was determined in terms of percent hemolysis using the following formula:

$$\text{Hemolysis \%} = \frac{A_{RBC_{540}}^t - A_{RBC_{540}}^{PBS}}{A_{RBC_{540}}^{TX-100} - A_{RBC_{540}}^{PBS}} \times 100$$

Where; $A_{RBC_{540}}^t$ is the absorbance read at 540 nm of RBC treated with the test compound, $A_{RBC_{540}}^{PBS}$ is the absorbance read at 540 nm of RBC treated with PBS, and $A_{RBC_{540}}^{TX-100}$ is the absorbance read at 540 nm of RBC treated with TritonX-100, respectively.

2.12. Effect of bare and streptomycin conjugated nanoparticles on the structural integrity of RBC

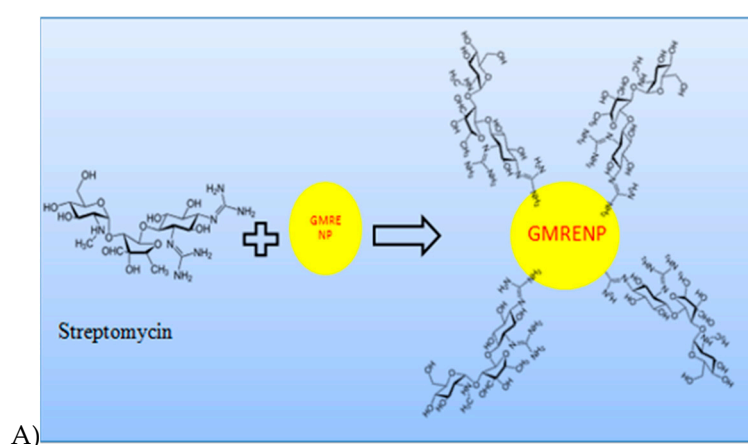
The effect of both bare and streptomycin conjugated metal nanoparticles on the human erythrocytes was analysed using light and scanning electron microscopic analyses. The samples for light microscopy were prepared by placing the cells on a clean glass slide covered with a coverslip and observed under a light microscope (Nikon Eclipse 80i upright microscope, Japan). For scanning electron microscopic analysis, the cells were prepared by fixing with 0.25% glutaraldehyde dissolved in 1x PBS (pH 7.4) and allowed to stand for 10 min at 37°C. Cells were collected by centrifugation at 1000 rpm for 5 min to minimize the possible mechanical rupture of the erythrocytes. The fixed samples were drop-coated and dried on aluminum foil and sputter-coated with gold (Hitachi E-1010 Ion sputter, Japan) for 60 sec and visualized under a scanning electron microscope (Hitachi, S-3400N, Japan).

3. Results

An attempt has been made in the current study to enhance the antibacterial activity of green synthesized metal nanoparticles by employing combinatorial therapy with antibiotics against the resistant pathogen. In this connection, the metal nanoparticles were synthesized from the rind extract of *G. mangostana* L., the obtained nanoparticles were subjected to a characterization study, and purification was done, as mentioned by Nisanthi et al. [18].

3.1. Bio-conjugation of streptomycin onto the green synthesized metal nanoparticles

The bioconjugation of streptomycin was carried out directly onto the surface of bare metal nanoparticles without using any functionalizing agents like amino acids, glutathione, and polyethylene glycol. A schematic diagram (Figure 1) shows the bio-conjugation of streptomycin onto metal nanoparticles.



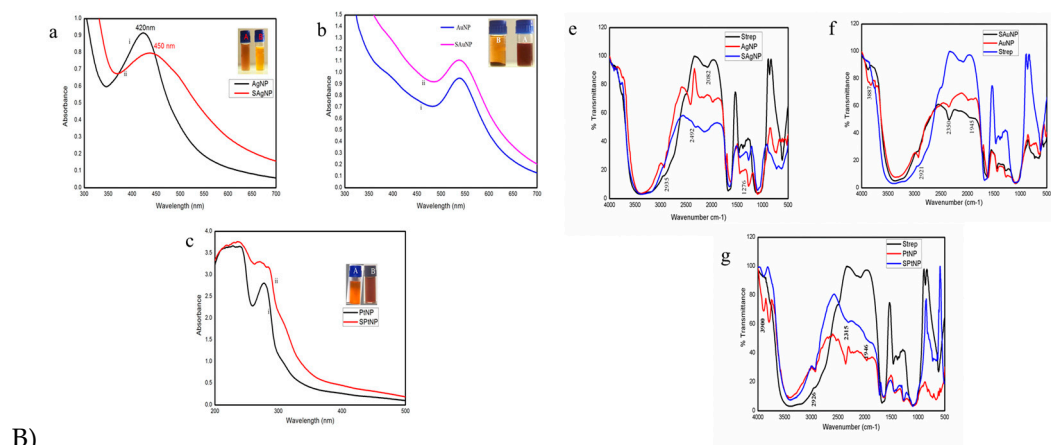


Figure 1. A) Schematic representation of bioconjugation of the drug Streptomycin onto the surface of green synthesized metal nanoparticles from the rind extract of *Garcinia mangostana* Linn. (AgNP, AuNP, and PtNP). B) UV-VIS spectral analysis of streptomycin conjugated onto the surface of silver (1. B) a-SAgNP), gold (1. B) b-SAuNP), and platinum (1. B) c-PtNP) nanoparticles [Inset: Turbidity induced by conjugation of streptomycin onto the nanoparticles (B) compared to bare nanoparticles alone (A)]; FT-IR spectral analysis of streptomycin, silver nanoparticles (AgNP), and nanoparticles conjugated with streptomycin (SAgNP) 1. B)-e; GNPs 1. B)-f; PtNPs 1. B)-g.

3.2. UV-VIS spectral analysis of streptomycin conjugated metal nanoparticles

UV-VIS spectral analysis indicated the characteristic shift in the SPR bands with all three nanoparticles conjugated with streptomycin. The SPR band shift for silver nanoparticles conjugated with streptomycin occurred at the wavelength range from 420 to 450 nm (SAgNP; Fig 1. B) a). The peak shift for gold nanoparticles occurred at 540 to 545 nm (SAuNP; Fig 1. B) b). The SPR band shift for platinum nanoparticles occurred from 260 nm (PtNP) to 263 nm (SPtNP; Fig 1. B) c).

3.3. FT-IR analysis of the streptomycin conjugated metal nanoparticles

The streptomycin conjugated on the surface of the metal nanoparticles was studied using the FT-IR spectral analysis. The characteristic bands observed for streptomycin and bare metal nanoparticles confirmed the conjugation of streptomycin onto the surface of the metal nanoparticles. The FT-IR spectrum showed bands at 2926, 2494, 1674, and 1465 cm^{-1} for streptomycin, which pertained to symmetrical and asymmetrical stretching of a methylene group, N-H stretching, C=C stretching of aromatic compounds, and -CH stretching vibration of atoms in AgNP (Figure 1(Be)), AuNP (Figure 1(Bf)) and PtNP (Figure 1(Bg)), respectively. The comparative FT-IR spectral analysis of the streptomycin conjugated silver (SAgNP; Figure 1(Be)), gold (SAuNP; Figure 1(Bf)), and platinum nanoparticles (SPtNP; Figure 1(Bh)) showed no changes in the absorption frequencies of other groups except the -N-H stretching peak, which broadened and shifted from a higher wavelength to a lower wavelength, and this confirmed the adsorption of streptomycin to the surface of the metal nanoparticles.

3.4. Evaluation of the antibacterial activity of streptomycin conjugated metal nanoparticles

The antibacterial activity of the bare green synthesized metal nanoparticles (AgNP, AuNP, and PtNP) and streptomycin conjugated metal nanoparticles (SAgNP, SAuNP, and SPtNP) were evaluated against streptomycin-resistant *Bacillus* sp. All three metal nanoparticles conjugated with streptomycin exhibited enhanced antibacterial activity compared to the bare metal nanoparticles. Remarkable enhancement (22 ± 0.3 mm) in the antibacterial activity of silver nanoparticles conjugated with streptomycin (SAgNP) was observed when compared to the antibacterial activity shown by the bare silver nanoparticles (14 ± 0.2 mm) and streptomycin preloaded disc impregnated with silver nanoparticles (16 ± 0.1 mm; Figure 2A & Table. 1). The bare gold and platinum nanoparticles did not show any antibacterial activity by themselves. However, the main antibacterial activity was observed

when the nanoparticles were conjugated with streptomycin. The zone of inhibition observed for gold and platinum nanoparticles conjugated streptomycin was 26 ± 0.1 and 23 ± 0.2 mm, respectively. The streptomycin preloaded discs impregnated with gold and platinum nanoparticles exhibited antibacterial activity, which was found to be equivalent, 13 ± 0.4 and 13 ± 0.2 mm, respectively (Figure 2B,C & Table. 1).

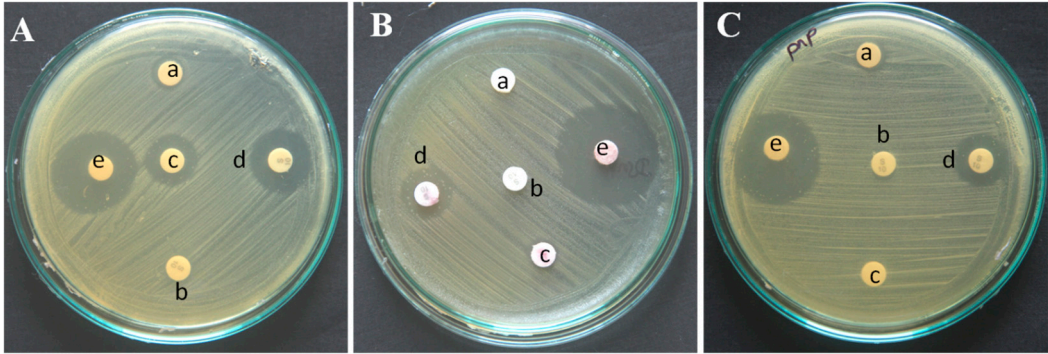


Figure 2. Antibacterial activity of the metal nanoparticles before and after conjugation with streptomycin against the streptomycin-resistant *Bacillus* sp. a: *G. mangostana* rind extract (GMRE); b: streptomycin; c: green synthesized AgNP (A), AuNP (B) and PtNP (C) nanoparticles; d: streptomycin preloaded disc impregnated with AgNP (A), AuNP (B) and PtNP (C) nanoparticles; e: streptomycin conjugated AgNP (A), AuNP (B) and PtNP (C) nanoparticles.

Table 1. Antibacterial activities of metal nanoparticles and streptomycin conjugated metal nanoparticles against streptomycin-resistant *Bacillus* sp.

Compounds used for testing the antibacterial activity	Zone of Inhibition (mm)		
	AgNP	AuNP	PtNP
GMRE	NZI	NZI	NZI
Streptomycin	NZI	NZI	NZI
Metal Nanoparticles	14 ± 0.2	NZI	NZI
Streptomycin preloaded disk impregnated with metal nanoparticles	16 ± 0.1	13 ± 0.4	13 ± 0.2
Streptomycin conjugated metal nanoparticle	22 ± 0.3	26 ± 0.1	23 ± 0.2

NZI: No zone of inhibition.

3.5. Determination of MIC of streptomycin conjugated metal nanoparticles

The minimum inhibitory concentration of the green synthesized silver nanoparticles (AgNP) and streptomycin conjugated silver nanoparticles were found to be 0.325 ppm and 0.187 ppm, respectively. The bare gold and platinum nanoparticles were highly insensitive against the streptomycin-resistant *Bacillus* sp. In contrast, the gold (SAuNP) and platinum (SPtNP) nanoparticles conjugated with streptomycin showed antibacterial activity, and the MIC determined was 0.1067 ppm and 34.00 ppm, respectively (Table S1).

3.6. Determination of the minimal bactericidal concentration (MBC) of streptomycin conjugated metal nanoparticles

Among the different test compounds, the bare silver nanoparticles (AgNP) exhibited an MBC at 0.65 ppm (Figure S1). In contrast, the bare AuNP (Figure S3) and PtNP (Figure S5) did not show antibacterial activity even when used at the highest possible concentrations. The MBC of streptomycin conjugated silver (SAgNP; Figure S2), gold (SAuNP; Figure S4), and platinum (SPtNP; Figure S6) nanoparticles was 0.375, 0.2135, and 68.0 ppm, respectively.

3.7. Determination of live/dead cells after treatment with streptomycin conjugated nanoparticles using AO/PI staining

The effect of streptomycin, bare, and streptomycin conjugated metal nanoparticles against streptomycin-resistant *Bacillus* sp. was evaluated by staining the cells with acridine orange and propidium iodide. The cells remained unaffected by streptomycin treatment (Figure 3B1) and fluoresced green when observed under the fluorescent microscope. The streptomycin-treated and untreated cells were also analyzed by propidium iodide staining, and no red fluorescence was observed (Figure 3A2,B2). The cells treated with bare and streptomycin conjugated nanoparticles resulted in the killing of the bacterial cells. The numbers of dead cells were comparatively higher in the cells treated with streptomycin conjugated silver nanoparticles (Figure 3D2) than in the silver nanoparticles treated cells. (Figure 3C2). The cells treated with bare gold nanoparticles did not kill the bacterial cells at all (Figure 3E1,E2) and the killing of the cells was prominent when treated with streptomycin conjugated gold nanoparticles (Figure 3F1,F2). Many cells with yellow fluorescence after the treatment with bare gold nanoparticles were observed (Figure 3E1), which did not show red fluorescence when the cells were stained with propidium iodide. The cells treated with bare platinum nanoparticles did not kill the bacterial cells (Figure 3G1,G2). In contrast, the treatment of streptomycin conjugated platinum nanoparticles killed the cells (Figure 3H1), increased number of dead cells was seen in the cells treated with streptomycin conjugated platinum nanoparticles (Figure 3H2).

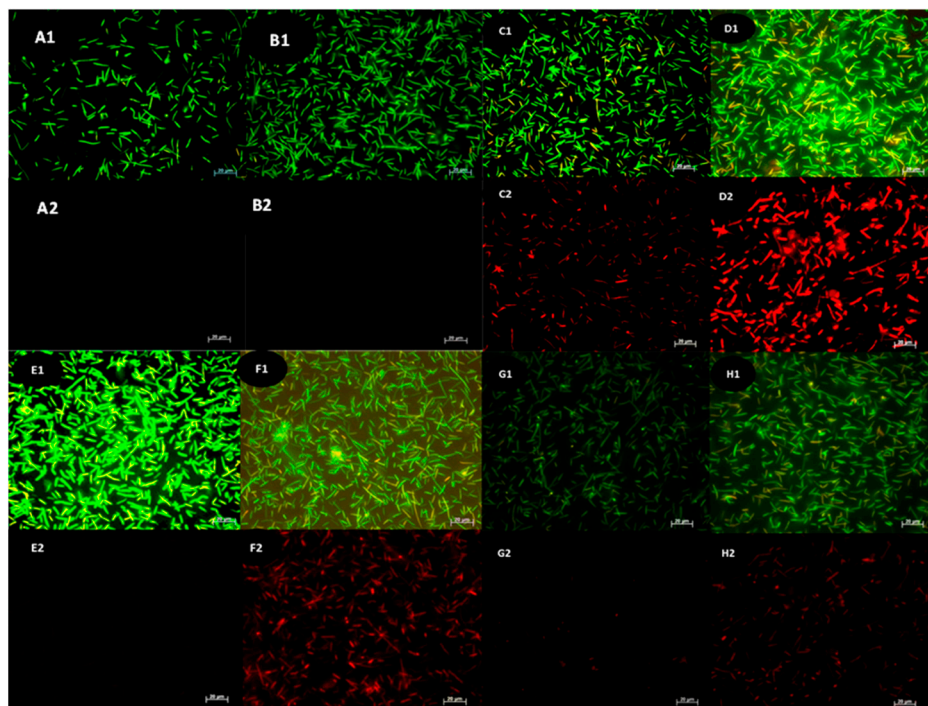


Figure 3. Determination of live/dead cells of *Bacillus* sp. after treatment with streptomycin (B1&B2), AgNP (C1&C2), SAgNP (D1&D2), AuNP (E1&E2), SAuNP (F1&F2), PtNP(G1&G2), and SPtNP (H1&H2). AO/PI dual stained cells: AO stained: control (A1) and streptomycin treated (B1) cells; AgNP (C1), SAgNP (D1), AuNP(E1), SAuNP(F1), PtNP(G1) and SPtNP(H1). Propidium iodide-stained control (A2) and streptomycin treated (B2) cells, AgNP (C2), SAgNP (D2), AuNP(E2), SAuNP(F2), PtNP(G2) and SPtNP(H2).

3.8. Cell viability analysis of cells treated with bare and streptomycin conjugated nanoparticles with FACS

Flow cytometry analysis was performed to determine the viability of the cells treated with bare and streptomycin conjugated nanoparticles. The bare AgNP and streptomycin conjugated metal nanoparticles (SAgNP, SAuNP, and SPtNP) killed the streptomycin-resistant *Bacillus* sp., and the

antibacterial activity AgNP- 92.64%, SAgNP-95.41%, SAuNP- 96.24, and SPtNP- 95.49%, respectively (Figure 4).

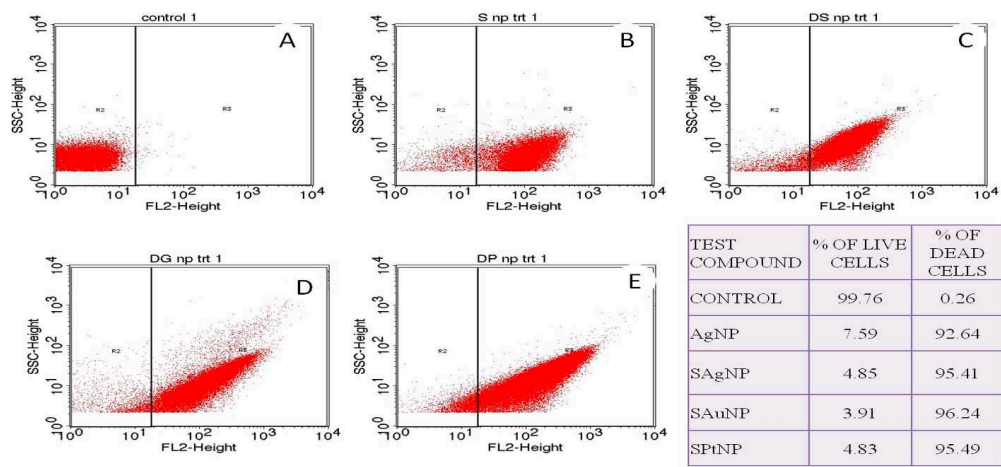


Figure 4. Fluorescence-activated cell sorting analysis of control (A), bare silver nanoparticles (MIC- 0.325ppm) (B), streptomycin conjugated, silver (MIC- 0.187ppm) (C), gold (MIC- 0.1067ppm) (D), and platinum (34ppm) (E) nanoparticles treated cells of *Bacillus* sp. Inset, the table shows the percentage of live and dead cells after the treatment at their respective minimum inhibitory concentration.

3.9. Effect of bare and streptomycin conjugated metal nanoparticles on the structural integrity of *Bacillus* sp.

The cells of *Bacillus* sp. treated with both bare (Figure 5b) and streptomycin conjugated silver nanoparticles (Figure 5c) resulted in lysis and disintegration. At the same time, the control cells remained intact (Figure 5a). The cells treated with bare gold nanoparticles did not affect the integrity of the cells (Figure 5d). In comparison, extensive lysis and damage of the cells were observed in those treated with streptomycin conjugated gold nanoparticles and appeared as a heap of granules (Figure 5e). Similarly, the cells treated with bare platinum nanoparticles (Figure 5f) did not cause any damage to the cells, and they remained intact. In contrast, extensive lysis occurred in the cells treated with streptomycin conjugated platinum nanoparticles (Figure 5g).

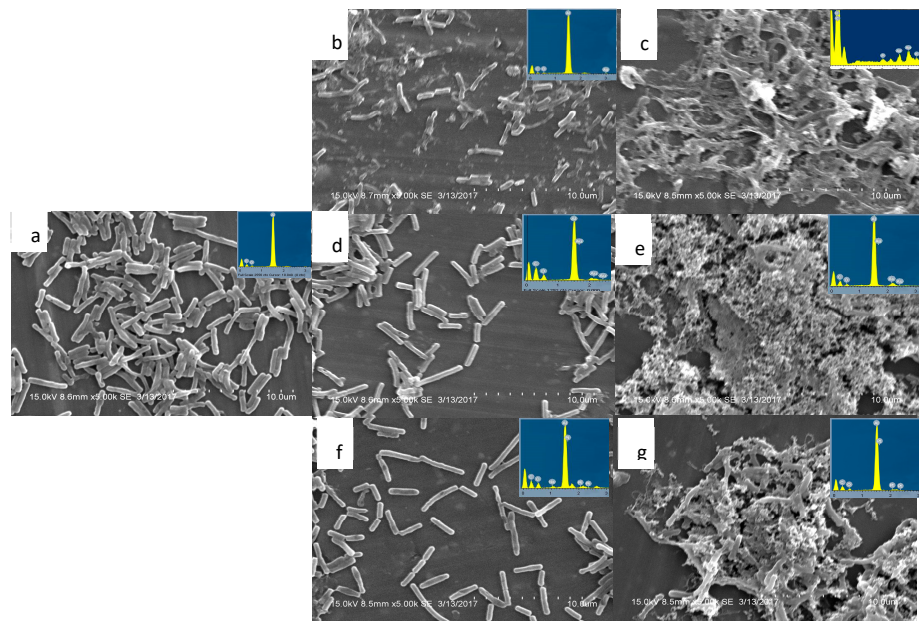


Figure 5. Scanning electron microscopic analysis of untreated cells of *Bacillus* sp. (a), cells treated with bare silver nanoparticles (b), cells treated with streptomycin conjugated silver nanoparticles (c), cells treated with bare gold nanoparticles (d), and cells treated with streptomycin conjugated gold

nanoparticles (e), cells treated with bare platinum nanoparticles (f), and cells treated with streptomycin conjugated platinum nanoparticles (g) with respective EDX analysis.

3.10. Effect of bare and streptomycin conjugated nanoparticles on the hemolysis of erythrocytes

The red blood cells treated with the bare green synthesized silver nanoparticles (AgNP) at 0.325, 0.1625, 0.08, and 0.04 ppm concentrations did not affect the cells. Whereas cells treated with 0.65 ppm resulted in lysis, and the solution turned red (Figure S8a), the percentage of lysis was calculated as 28%. No lysis was observed when the cells were treated with the bare AgNP, AuNP, and PtNP and streptomycin conjugated SAgNP, SAuNP, and SPtNP nanoparticles at their minimum inhibitory concentrations (Figure S8a,b).

3.11. Effect of bare and streptomycin conjugated nanoparticles on the structural integrity of RBC

The red blood cells treated with PBS (pH 7.4) appeared in their characteristic biconcave discoid shape (Figure 6a), whereas the cells treated with Triton X-100 resulted in complete disintegration and were morphologically quite distinct. A few swollen cells with spikes on the surface (echinocyte-like) were also observed, generally termed ghost cells. The presence of many ghost cells was spotted in the sample treated with Triton X-100 (Figure 6b). The RBCs treated with the MIC concentration of bare silver nanoparticles at 0.325 ppm (Figure 6c) and streptomycin conjugated silver nanoparticles at 0.1875 ppm (Figure 6d), gold nanoparticles at 0.106 ppm (Figure 6f), and platinum nanoparticles at 34 ppm (Figure 6h) did not have any effect on the structural integrity of RBC. They were similar to what was observed in the negative control. The bare green synthesized gold (AuNP), and platinum (PtNP) nanoparticles did not cause any morphological changes even when they were used at their highest concentration, 127 and 235 ppm, respectively (Figure 6e,f).

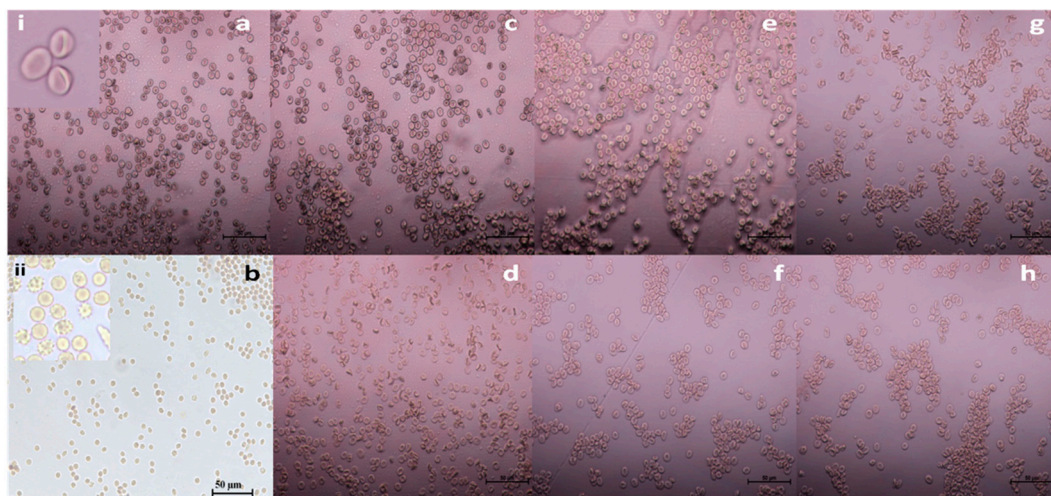


Figure 6. Effect of bare and streptomycin conjugated nanoparticles on the structural integrity of RBC's (a) PBS; (b) Triton X – 100; (c) AgNP (0.325 ppm); (d) SAgNP (0.187 ppm); (e) AuNP (127 ppm); (f) SAuNP (0.106 ppm), (g) PtNP (235 ppm); (h) SPtNP (34 ppm). (40X). Insets: (i) RBC with biconcave smooth surface; (ii) Appearance of ghost cells following treatment with Triton X - 100.

The RBCs were viewed under a scanning electron microscope to visualize any significant structural change by the synthesized nanoparticle exerted on RBC. The cells treated with Triton X-100 resulted in deformation and aggregation (Figure 7b), while the cells in PBS-treated control showed the characteristic biconcave with a smooth wall (Figure 7a). The RBCs were treated with bare (AgNP, AuNP, and PtNP; Figure 7c,e,g) and streptomycin conjugated (SAgNP, SAuNP, and SPtNP; Figure 7d,f,h) nanoparticles showed the typical characteristic doughnut-shaped cells. However, these cells were found to have adhered nanoparticles uniformly distributed all over the cells. The RBCs treated with nanoparticles showed no aberrant morphological cells. Still, the appearance of small

uniform-sized particles on the surface of RBC was found equivalently in all treated samples, which indicates the presence of nanoparticles on the surface of the RBC.

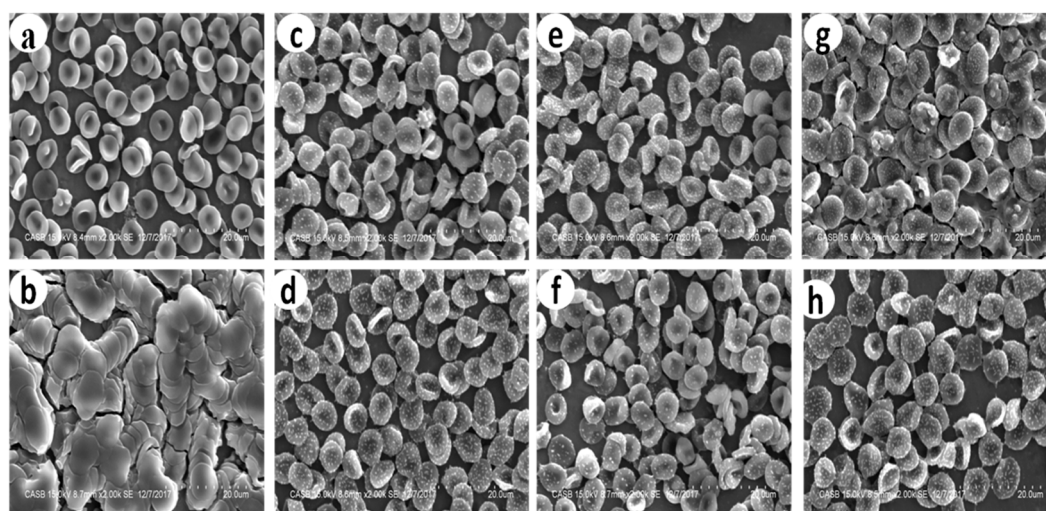


Figure 7. Effect of bare and streptomycin conjugated nanoparticles on the structural integrity of RBC's under scanning electron microscope a: PBS; b: Triton X – 100; c: AgNP (0.325 ppm); (d) SAgNP (0.187 ppm); e: AuNP (127 ppm); f: SAuNP (0.106 ppm), g: PtNP (235 ppm); h: SPtNP (34 ppm).

4. Discussion

The prevalence of antibiotic-resistant microorganisms to multiple antibiotics coupled with the increasing healthcare cost has propelled researchers to develop new and cost-effective antimicrobial reagents. This development has led to the resurgence of metals used in ancient times since microorganisms did not develop resistance against these metals. Combinatorial therapy joining one or more drugs, is the most exciting area of research to combat multidrug-resistant pathogens. Combinatorial therapy has a potential track record concerning a broader antimicrobial spectrum, synergistic effect, and reduced risk for emerging resistance during therapy compared to monotherapy. In the absence of evidence-based treatment options, combinations are increasingly employed to enhance the antibacterial effects of available drugs [23]. However, due to the continuous misuse of antibiotics, the development of resistance and adverse effects associated with it can occur. A case study conducted by Paul et al. has compared the monotherapy's effectiveness with combinatorial therapy consisting of aminoglycoside and β -lactam in patients with sepsis where bacterial resistance was frequently encountered [24]. They found that the continual use of combinatorial therapy was not associated with mortality but led to nephrotoxicity in patients.

Combinatorial therapy is considered a double-edged sword, so its usage must be strictly restricted to multi-drug-resistant bacteria [25]. Streptomycin-resistant bacteria have been treated with streptomycin conjugated metal nanoparticles in place of β -lactam. The following observations have been made from this study:

1. The mechanism of action of metal nanoparticles is similar to β -lactam antibiotics against bacteria.
2. The enhanced potential of combinatorial therapy consists of aminoglycoside antibiotics with metal nanoparticles to treat aminoglycoside-resistant bacteria.

Therefore, an attempt has been made in the present investigation to evaluate the antibacterial activity of bare metal nanoparticles [26–28] and metal nanoparticles conjugated with streptomycin.

The results obtained in the present investigation for the first time demonstrated enhanced bactericidal activity of the green synthesized silver (AgNP), gold (AuNP), and platinum (PtNP) nanoparticles when they were conjugated with the streptomycin compared to their free forms. Generally, such conjugation needs the process of functionalization and high energy requirements.

Ramulu et al. (2015) [29] synthesized the silver nanoparticles after the reduction of 2 mM silver nitrate with 0.6 mM NaBH_4 , followed by biofunctionalization with antibacterial peptide polymyxin-B. Similarly, [30] have synthesized aminoglycoside gold nanoparticles by adding trisodium citrate to 1mM chloroauric acid, followed by adding 3 mM drug to the citrate-capped gold nanoparticles under stirring conditions for two h continuously. Hydrolysable linkers have been used to conjugate Human Serum Albumin nanoparticles with two antineoplastic agents, imatinib and 5-fluorouracil [31]. 1-Ethyl-3-(3-dimethyl aminopropyl) carbodiimide (EDC) has been used as an agent to link the 5-fluorouracil with green synthesized gold nanoparticles synthesized from the peel extract of *Punica granatum* with folic acid [32]. In the present study, no such chemical interference has been utilized as a functionalizing agent in determining the bio-conjugated nanoparticles' bactericidal activity of the bioconjugated nanoparticles to avoid the adverse effect of chemicals [33].

The UV-VIS spectral analysis of the streptomycin conjugated metal nanoparticles, such as SAgNP, SAuNP, and SPtNP, has suggested that the metal nanoparticles' integrity was not compromised even after the bio-fabrication with the drug. The decreased aggregation observed with the streptomycin conjugated metal nanoparticles further points to the presence of streptomycin on the surface of metal nanoparticles. Adsorption appears to be the interaction between the antibiotics and nanoparticles, as is evident from the redshift in the surface plasmon resonance in the spectrum. This phenomenon indicates the formation of the larger nanoparticles; however, the shift is less than ~3 nm in the case of SPtNP (Figure 2c), 10 nm in the case of SAuNP (Figure 2b), and 30 nm in the case of SAgNP (Figure 2a) when compared to their bare nanoparticles. A similar observation was made by Debalina et al. [34] when the gold nanoparticles synthesized with sodium borohydride as the reducing agent was conjugated with ampicillin, streptomycin, and kanamycin. The surface plasmon resonance observed for the bare gold nanoparticles was 526 nm. The conjugation of antibiotics with nanoparticles leads to the formation of larger particles, as evidenced by the color change from red wine to purple. The redshift observed suggested the adsorption of the antibiotics onto the surface of the nanoparticles. It is well known that an antibiotic molecule's the presence of hydroxyl and amine groups of an antibiotic molecule can easily protonate in an acidic or neutral solution, transfer the electrons to the metal ions and form metal-amine complexes via simple amine chemistry [35].

The FT-IR spectrum is the fingerprint for identifying unknown compounds compared to previous reference spectra [36]. The alteration in frequency and intensity observed between the bare metal nanoparticles and streptomycin conjugated metal nanoparticles is due to the change in the atom vibration. Nirmala and Pandian [30] have suggested that the drug aminoglycoside contains active groups which can efficiently react with gold nanoparticles by chelation and get adsorbed onto the surface. The antimicrobial entity comes near the nanogold core surrounded by aminoglycoside drug moieties. In the present study, spectral analysis of streptomycin and streptomycin conjugated metal nanoparticles (SAgNP, SAuNP, and SPtNP) suggests a possible alteration in the vibration of the atom, and the change in the -NH band stretch indicates the involvement of the amine group of streptomycin in the conjugation process where the chemical structure of the drug left unaltered. However exact nature of events during the conjugation process in the present study is far from satisfactory and warrants rigorous analyses to explain the phenomenon behind the conjugation.

The antibacterial activity of bare green synthesized nanoparticles (AgNP, AuNP, and PtNP), streptomycin preloaded disk impregnated with green synthesized metal nanoparticles, and streptomycin conjugated metal nanoparticles (SAgNP, SAuNP, and SPtNP) have been performed against the streptomycin-resistant *Bacillus* sp. by disk diffusion method. There was a remarkable increase in antibacterial activity when the antibiotic streptomycin was conjugated with a silver nanoparticle (22 mm); however, the antibacterial activity observed with a streptomycin preloaded disk impregnated with silver nanoparticle showed only a marginal increase in activity (16 mm) from the bare silver nanoparticles (14 mm). In terms of percentage, the highest (37.5%) antibacterial activity was observed with streptomycin conjugated silver nanoparticles (SAgNP), followed by streptomycin preloaded disk impregnated with silver nanoparticles (14%) over the bare silver nanoparticles. Interestingly, the streptomycin conjugated gold (SAuNP) and platinum (SPtNP) nanoparticles have shown a 100 and 76% increase in antibacterial activity, respectively, when compared to the activity

shown by the same nanoparticles when added to streptomycin preloaded discs. Thus, it is evident that the enhancement of the antibacterial activity is due to the conjugation of streptomycin onto the nanoparticles (Table 1).

One essential property of any antibacterial agent is determining its minimal inhibitory concentration, allowing it to be used in a clinical setup. The minimum inhibitory concentration (MIC) is defined as the lowest concentration of an antimicrobial agent that inhibits the visible growth of bacteria. This information will be quite valuable during the antibacterial agent's research and development phase of an antibacterial agent to determine the appropriate concentrations required in the final product. These drug concentrations are needed to produce the effect; ordinarily several hundred to a thousand times less than the concentration found in the final finished dosage form. The minimum bactericidal concentration (MBC) is the lowest concentration of an antibacterial agent required to kill a bacterium over a fixed period of 18 or 24 h, under a specific set of conditions. It can be determined by sub-growing the bacterium previously incubated with the antibiotics on an agar medium after appropriate dilutions.

It has been observed in the present study that the streptomycin-resistant *Bacillus* sp. was found to be highly resistant to free streptomycin and bare gold and platinum nanoparticles (Figure S1). However, the same bacterium became susceptible when treated with the bare and streptomycin conjugated metal nanoparticles in a dose-dependent manner (Table S1). Among the conjugated nanoparticles, the gold nanoparticle with streptomycin showed the lowest MIC (0.106 ppm) followed by SAgNP (0.187 ppm) and SPtNP (34.0 ppm).

The turbidity caused by the insoluble compounds during broth dilution has been observed to lead to false-positive results. Therefore, the MBC was determined by culturing on Muller Hinton agar medium. The agar medium incorporated with a particular concentration of test compound where no visible growth occurred was determined as the minimum bactericidal concentration (MBC). The MBC's of AgNP, SAgNP, SAuNP, and SPtNP was found to be 0.65, 0.375, 0.2135, and 68 ppm, respectively.

It has become essential to distinguish a compound's bactericidal or bacteriostatic activity of a compound. Woods and Washington [37] have described an antimicrobial agent as bactericidal when the MBC/MIC ratio is less than or equal to 4, and bacteriostatic when the ratio is greater or equal to 16. Thus, the MBC/MIC ratio is a parameter that reflects the bactericidal capacity of the analyzed compound [38]. In the present study, the tolerance level of the test bacterium was determined by analyzing the ratio of MBC/MIC, and the ratio of all the analyzed antimicrobial agents such as AgNP, SAgNP, SAuNP, and SPtNP was found to be surprisingly 2, i.e., the MBC is double the concentration of MIC, suggesting that the compound could be potential antibacterial agents against streptomycin-resistant *Bacillus* sp. Whereas SAuNP and SPtNP exhibited antibacterial activity only after conjugating the streptomycin with the bare nanoparticles, suggesting that the nanoconjugates increased the antibacterial property of streptomycin by acting as a nanocarrier of the drug to the target site. The results obtained in the present study have been in line with the observations made by Das et al. [38]; they evaluated the antibacterial activity of silver nanoparticles synthesized from the leaf extract of *O. gratissimum* against multidrug-resistant *E. coli* and *S. aureus* strains. The obtained MIC for *E. coli* was 4 µg/ml and for *S. aureus* was 8 µg/ml, and the MBC was two times higher than the MIC, which was 8 and 16 µg/ml, respectively, for the organisms.

After treatments, the intact and compromised cells can be distinguished by staining the treated cells with AO/PI staining and viewing them under a fluorescent microscope. The membrane integrity of the bacteria treated with the antimicrobial test compounds has also been analyzed using acridine orange and propidium iodide staining [39]. The stains used were the membrane-impermeable PI causing red fluorescence in cells with compromised membranes. AO is a cell-permeable nucleic acid binding green fluorescent dye that enters the cells regardless of whether they are intact or compromised. The live/undamaged cells will appear green, whereas bacteria with compromised cell walls will appear reddish-orange, and the dead cells will appear red. The streptomycin-resistant *Bacillus* sp was treated with the respective MIC of tested antimicrobial compounds. The cells with compromised cell walls allow the PI stain to get through the cell wall due to the lack of cell wall

integrity, and thus the PI stains the nucleic acid (DNA) and appears red when viewed under a fluorescence microscope. The number of red fluorescent cells was higher in the case of SAgNP, SAuNP, and SPtNP treated cells than in AgNP treatment.

Accurate determination of live and dead bacteria is vital in determining the dosage level of antibiotics. The traditional culture-based viable test does not provide real-time results needed in applications such as industrial manufacturing. However, the enumeration of accurate live and dead cells is now possible with flow cytometric analyses. The nucleic acid leaked out due to the treatment will be freely available for the PI dye for binding, leaving the cells available to emit red fluorescence, and thus enumeration of the dead cells is possible by flow cytometric technique. In the present study, the cells were treated with their MIC concentration, and the numbers of dead cells were enumerated, and 96% of cells were found dead at 0.106 ppm, 95% at 0.18, and 34 ppm for SAgNP and SPtNP, respectively. About 92% of dead cells were found at 0.325 ppm in respect of AgNP treatment.

Scanning electron micrographs representing the ultrastructure of cells are a powerful method for understanding the effect of nanoparticles and have been widely described in the literature. An earlier observation made by Das et al. [38,40] has shown damaged membranes of bacterial cells when treated with silver nanoparticles synthesized from the extract of *O. gratissimum*, which resulted in enhanced plasma membrane permeability of the plasma membrane. This permeability has led to the leakage of cellular content and the death of the cells [41].

The present study has also attempted to evaluate the structural changes after challenging the bacterium with antibiotic-conjugated nanoparticles using electron microscopic analysis. The cells treated with silver nanoparticles showed extensive damage to the structure (Figure 5b). Most cells were disintegrated and lysed. The cells treated with gold (AuNP) and platinum (PtNP) nanoparticles, however, did not have any effect on the integrity of the structure (Figure 5b,d).

The exact mechanism by which the nanoparticles penetrate the bacteria is not fully understood. However, according to Morones et al. [42], silver nanoparticles can damage the cells by interacting with phosphorous and sulfur-containing compounds such as DNA and regulating enzymes. In the present study, the silver nanoparticles (AgNP) alone have shown the potential to damage the bacterial cells by creating small pits on the surface and penetrating the cells, which causes the leakage of intracellular compounds and eventually leads to the death of the bacteria. The failure of gold (AuNP) and platinum (PtNP) nanoparticles may be due to the lack of affinity towards phosphorus and sulfur-containing compounds compared to silver. The gold /platinum nanoparticles are higher-order metals used as biocompatible catalyst and drug delivery agents because of their inertness. However, the inert gold and platinum nanoparticles, when conjugated with streptomycin, have acquired remarkable antibacterial activity and were able to lyse the cells (Figure 5e,g), ultimately leading to death. In general, antibiotic resistance against the aminoglycoside class of antibiotics by bacteria can be trespassed by combining with the β -lactam class of drugs. With this crucial point in mind, we can understand the mechanism of the nanoparticle, where the nanoparticle acts as the agent to damage the bacteria's cell wall of the bacteria and carries the streptomycin inside the cells, and then it acts on the protein machinery leading to the death of the bacteria.

One of the most critical challenges in the growing field of nanomedicine is the behavioral nature of nanoparticles inside the cells. Metabolic and immunological responses induced by the nanoparticles are still under investigation; however, they may act as checkpoints for the growth of nanomedicine. Nanotoxicology has been described as the discipline that deciphers the molecular events that regulate nanoparticle bioaccumulation and toxicity [43]. There must be enhanced vigilance on the potential secondary effects generated by using nanomaterials in nanomedicine. Blood is the major component in humans that serves as the primary route for the translocation of foreign bodies into cells, tissues, and organs. Therefore, its compatibility with foreign bodies assumes significance in developing materials like nanoparticles into effective antimicrobial agents.

RBC is an essential component of the blood circulatory system since it plays a crucial role in transporting oxygen to the body tissues. Any malfunction or disruption of the RBC might pose a risk to the health; therefore, the need to test the influence of the nanoparticles on RBC is inevitable. Though it is considered to be the most crucial area of research, there have been only a few reports

available on the hemocompatible nature of the nanoparticles, such as silica [44],[45], TiO₂ [46], and polymer nanoparticles [47].

In the present study, an attempt has been made to assess the hemocompatible nature of the bare and streptomycin conjugated silver, gold, and platinum nanoparticles synthesized from the rind extract of *G. mangostana* fruit. It has been observed that no hemolysis was induced either by the bare nanoparticles or streptomycin conjugated nanoparticles (Figure S8).

Investigations undertaken to assess the hemocompatible nature of gold nanoparticles have shown that they are biocompatible and can be used as nanomedicine. It has been found that the gold nanoparticles synthesized from the extract of *Zinger Officinale* caused very little (0.2%) hemolysis, even at the highest concentration of 10 mg/ml. [48]. Similarly, the silver nanoparticles synthesized from β -glucan isolated from the edible mushroom, *Pleurotus Florida*, showed hemocompatibility despite antibacterial activity against the multi-antibiotic resistant bacteria (MAR) *K. pneumonia* YSI6A[49]. The RBC treated with silver nanoparticles at 15 μ g/ml concentration induced only 0.68 % of hemolysis and was found to be hemocompatible. The MIC for the particular bacterium was found to be 40 μ g/ml, which is ~2 times higher than the LD₅₀ concentration however found to be compatible with RBC. The percentage of hemolysis of platinum nanoparticles synthesized from the extract of seaweed, *Padina gymnospora* reported as 13% for 40 μ g/ml [50].

The silver nanoparticles synthesized from *Catharanthus roseus* have caused hemolysis at 10 μ g/ml; however, the concentration from 1 to 5 μ g/ml has been considered safe on RBC [51]. Srinath et al. [52] synthesized gold nanoparticles from the bacterium *Brevibacillus formosus* and showed them to have no hemolytic activity even at the highest concentration (150 and 200 μ g/ml). The hemocompatible nature of the gold nanoparticles synthesized from the tuber extract of *Curcuma mangga* has also been investigated recently [53]. The percentage of hemolysis increased when the concentration of the gold nanoparticles increased, and the observed percentages were 2.7, 1.8, 2.6, 6.2, and 9.9%, with 3.13, 6.25, 12.5, 25, and 50 μ g/ml, respectively.

Asharani et al. [54] have observed that the platinum and gold nanoparticles caused no hemolysis and hemagglutination, whereas silver nanoparticles caused hemolysis [55]. They synthesized four different types of nanoparticles through the chemical method and investigated the effect of those nanoparticles on the surface of human erythrocytes. It has been suggested that the membrane damage in the nanoparticle-treated cells led to the lysis of RBC, damaging the adjacent normal cell through DNA damage [56]. The results obtained in the present study are in good agreement with the above research. In the present research, the silver nanoparticles (AgNP) synthesized from the rind extract of *G. mangostana* fruit alone showed hemolysis at a higher concentration (0.65 ppm). In comparison, no hemolysis occurred at a lower concentration. Gold and platinum nanoparticles were comparatively more hemocompatible than the silver nanoparticles synthesized from the same source (Figure S8a).

The electron microscopic analysis of cells treated with platinum nanoparticles (PtNP) revealed the presence of a few ghost cells and the slight alteration in the shape of RBC from discocyte to spherocyte (Figure 7g). Continuous exposure might have led to the loss of the membrane's resilience and flexibility. Further investigation is necessary to ascertain the nature of the effect before this can be taken for any clinical trial.

Interestingly, the RBC treated with bare and streptomycin conjugated gold nanoparticles (Figure 7e,f) showed no sign of morphological disturbances, which suggests that these conjugates could be used against the multidrug-resistant bacteria without causing any effect on the normal cells (Figure 7a).

5. Conclusions

Bio-fabrication of streptomycin onto green synthesized noble metal nanoparticles synthesized from the aqueous rind extract of *G. mangostana* fruit has been achieved, which could be considered the most cost-effective drug modification methodology. The streptomycin conjugated nanoparticles were characterized using UV-VIS and FT-IR spectral analyses. The addition of streptomycin to the nanoparticles caused a solution color change and showed a shift in the absorption spectra from 420 to 450 nm for SAgNP, 540 to 545 nm for SauNP, and 260 to 263 nm for SPtNP when analysed with

UV-VIS spectroscopy. The shift in the wavelength confirms the successful conjugation between the streptomycin and the metal nanoparticles. The FT-IR spectra obtained for sAgNP, SAuNP, and SPtNP have shown that the $-NH$ stretching of the streptomycin was responsible for attachment on the surface of the metal nanoparticle and maintaining the chemical structure of the drug even after conjugation. The antibacterial activity of the streptomycin-conjugated metal nanoparticles (sAgNP, SAuNP & SPtNP) and the streptomycin preloaded disk impregnated with nanoparticles was evaluated by the disk diffusion method. The streptomycin conjugated gold nanoparticle (SAuNP) showed a 100 % antibacterial activity compared with the AuNP alone, while the streptomycin conjugated silver and platinum nanoparticles showed a 22 and 76 % increase, respectively. The minimum inhibitory concentration of AgNP and SAgNP was determined as 0.325 and 0.187 ppm, respectively. The MIC value observed with streptomycin conjugated silver nanoparticles was 46% lesser when compared with the value observed with bare nanoparticles. The MIC of streptomycin conjugated gold and platinum nanoparticles were found to be 0.1067 and 34.0 ppm, respectively. The minimum bactericidal concentration of AgNP, sAgNP, SAuNP, and SPtNP were determined as 0.65, 0.375, 0.2135, and 68 ppm, respectively. The test compounds' respective MIC and MBC values determined the tolerance level of streptomycin-resistant *Bacillus sp.* The ratio of MBC/MIC for AgNP, SAgNP, SAuNP, and SPtNP was 2.0, suggesting that these compounds are bactericidal in nature. After treating them with streptomycin conjugated nanoparticles, the number of live and dead bacteria after treating them with streptomycin conjugated nanoparticles was calculated using flow cytometric analysis. 96% of cells were found dead upon treatment with SAuNP, while 92 and 95 cells were found dead upon treatment with AgNP and SAgNP, respectively. About 95% of cells were found dead upon treatment with SPtNP. The cells treated with streptomycin conjugated nanoparticles showed lysis and fragmentation, suggesting that the streptomycin conjugated nanoparticles could be an ideal agent for treating drug-resistant bacteria in a clinical setup. The hemocompatibility of bare and streptomycin conjugated metal nanoparticles was evaluated with human erythrocytes. No hemolysis was observed when the RBC was treated with silver nanoparticles at its MIC of 0.325 ppm. Cells treated with higher concentrations (0.65 ppm) were rendered hemolytic to 28%. No hemolysis was observed when the cells were treated with AuNP, PtNP, SAgNP, SAuNP, and SPtNP, even when they were used at their highest concentration. Light microscopic analysis of RBC treated with the test compounds showed no sign of aggregation, while the formation of many ghost cells was observed in the cells treated with Triton X-100. Scanning electron microscopic analysis of RBC treated with bare and streptomycin conjugated nanoparticles has shown the characteristic biconcave cells with smooth surfaces suggesting the hemocompatibility nature of the test compounds.

This present investigation opens a new avenue of research for the cost-effective green synthesis of metal nanoparticles from agricultural waste, which can be considered as the value-added product, and the conjugation of the drug onto the surface of the metal nanoparticles without any harmful interfacing agents projects this study as a unique and novelty. Moreover, the emergence of multidrug resistance in pathogenic organisms has caused growing concern, especially among healthcare providers, which necessitated the development of new antimicrobial compounds. Antibiotic resistance keeps increasing in frequency, with all major classes of antibiotics used to treat a wide variety of diseases. The development of resistance against metal nanoparticles is more challenging for any pathogen. Thus, an effort has been made in the present investigation and proves a new formulation of drugs by conjugating the commercial drug with nanoparticles to treat microbial resistance.

Supplementary Materials: The following supporting information can be downloaded at the website of this paper posted on Preprints.org.

Author Contributions: N. Ramasami: Conceptualization, Methodology, Investigation, Writing – Original Draft. M. Dhayalan: Supervision, Writing- Review and Editing. M. Selvaraj: Formal Analysis, Data Curation. S. U. Mohammed Riyaz: Formal Analysis, Data Curation. Rajakumar K. Dmitry Zhrebtsov: Data curation; J. C. Mejuto: Supervision; P. Palani: Supervision, Writing – Review and Editing. J. Simal- Gandara: Supervision, Writing – Review and Editing. A. Cid-Samamed: Formal analysis, Supervision, Writing - Review and Editing.

Funding: Funding for open access charge: Universidade de Vigo/CISUG. The author, R.N, expresses thanks to the Department of Science and Technology for the financial support of INSPIRE Senior Research Fellowship (SRF) and the Director, CAS in Botany, for providing the necessary facilities to carry out the work. The authors also thank the National Centre for Nanoscience and Nanotechnology, the University of Madras for HR-TEM analyses, SAIF-IIT Madras for FT-IR analyses, and SRM-IST for FACS analyses.

Data Availability Statement: not applicable.

Conflicts of Interest: The authors declare no conflict of interest.

References

1. Neu, H.C. The Crisis in Antibiotic Resistance. *Science* (1979) **1992**, 257, 1064–1073, doi:10.1126/science.257.5073.1064.
2. Criswell, D.; Fleming, A.; Ii, W.W.; Criswell, D.; Biology, M. The Evolution of Antibiotic Resistance. *Acta Facts* **2004**, 33, 1–4.
3. Neu, H.C. The Crisis in Antibiotic Resistance. *Science* (1979) **1992**, 257, 1064–1073.
4. Neu, H.C.; Gootz, T.D.; Baron, Samuel. Chapter 11: Antimicrobial Chemotherapy. In *Medical Microbiology*; University of Texas Medical Branch, 1996; p. 1273.
5. Harold C. Neu and Thomas D. Gootz. General Antimicrobial Chemotherapy Available online: <https://www.ncbi.nlm.nih.gov/books/NBK7986/?report=printable>.
6. Bakshi, M.S. Nanotoxicity in Systemic Circulation and Wound Healing. *Chem Res Toxicol* **2017**, 30, 1253–1274.
7. Pan, D.; Vargas-Morales, O.; Zern, B.; Anselmo, A.C.; Gupta, V.; Zakrewsky, M.; Mitragotri, S.; Muzykantov, V. The Effect of Polymeric Nanoparticles on Biocompatibility of Carrier Red Blood Cells. *PLoS One* **2016**, 11, doi:10.1371/journal.pone.0152074.
8. Qiang Chen, L.; Fang, L.; Ling, J.; Zhi Ding, C.; Kang, B.; Zhi Huang, C. Nanotoxicity of Silver Nanoparticles to Red Blood Cells: Size Dependent Adsorption, Uptake, and Hemolytic Activity. **2015**, doi:10.1021/tx500479m.
9. Chen, L.Q.; Fang, L.; Ling, J.; Ding, C.Z.; Kang, B.; Huang, C.Z. Nanotoxicity of Silver Nanoparticles to Red Blood Cells: Size Dependent Adsorption, Uptake, and Hemolytic Activity. *Chem Res Toxicol* **2015**, 28, 501–509, doi:10.1021/tx500479m.
10. Fattah, B.; Arif, · Huner; Hamzah, · Haider Antimicrobial and Antibiofilm Activity of Biosynthesized Silver Nanoparticles Against Beta-Lactamase-Resistant Enterococcus Faecalis. **2010**, doi:10.1007/s12010-022-03805-y.
11. Godoy-Gallardo, M.; Eckhard, U.; Delgado, L.M.; de Roo Puente, Y.J.D.; Hoyos-Nogués, M.; Gil, F.J.; Perez, R.A. Antibacterial Approaches in Tissue Engineering Using Metal Ions and Nanoparticles: From Mechanisms to Applications. *Bioact Mater* **2021**, 6, 4470–4490, doi:10.1016/j.bioactmat.2021.04.033.
12. Ajingi, S.; Jongruja, N. Antimicrobial Peptide Engineering: Rational Design, Synthesis, and Synergistic Effect. *Russ J Bioorg Chem* **2020**, 46, 463–479, doi:10.1134/S1068162020040044.
13. Nainu, F.; Permana, A.D.; Juniarti, N.; Djide, N.; Anjani, Q.K.; Utami, R.N.; Rumata, N.R.; Zhang, J.; bin Emran, T.; Simal-Gandara, J. Antibiotics Pharmaceutical Approaches on Antimicrobial Resistance: Prospects and Challenges. **2021**, 10, doi:10.3390/antibiotics10080981.
14. Mohammed, A.B.A.; Hegazy, · A E; Salah, · Ahmed Novelty of Synergistic and Cytotoxicity Activities of Silver Nanoparticles Produced by Lactobacillus Acidophilus. *Appl Nanosci* **2021**, 1, 3, doi:10.1007/s13204-021-01878-5.
15. Ali Hussein, H.; Fitrya Syamsumir, D.; Aisha Mohd Radzi, S.; Yong Fu Siong, J.; Atikah Mohamed Zin, N.; Azmuddin Abdullah, M. Phytochemical Screening, Metabolite Profiling and Enhanced Antimicrobial Activities of Microalgal Crude Extracts in Co-Application with Silver Nanoparticle. *Bioresour. Bioprocess* **2020**, 7, 39, doi:10.1186/s40643-020-00322-w.
16. Hashem, A.H.; Shehabeldine, A.M.; Ali, O.M.; Salem, S.S. Citation: Hashem, A Synthesis of Chitosan-Based Gold Nanoparticles: Antimicrobial and Wound-Healing Activities. **2022**, doi:10.3390/polym14112293.
17. Yu, X.; Li, J.; Mu, D.; Zhang, H.; Liu, Q.; Chen, G. Green Synthesis and Characterizations of Silver Nanoparticles with Enhanced Antibacterial Properties by Secondary Metabolites of Bacillus Subtilis (SDUM301120). **2021**, doi:10.1080/17518253.2021.1894244.
18. Nishanthi, R.; Malathi, S.; S., J.P.; Palani, P. Green Synthesis and Characterization of Bioinspired Silver, Gold and Platinum Nanoparticles and Evaluation of Their Synergistic Antibacterial Activity after Combining with Different Classes of Antibiotics. *Materials Science and Engineering: C* **2019**, 96, 693–707, doi:10.1016/j.msec.2018.11.050.
19. Chakraborty, S.P.; Sahu, S.K.; Mahapatra, S.K.; Santra, S.; Bal, M.; Roy, S.; Pramanik, P. Nanoconjugated Vancomycin: New Opportunities for the Development of Anti-VRSA Agents. *Nanotechnology* **2010**, 21, 105103, doi:10.1088/0957-4484/21/10/105103.

20. Mohammed Fayaz, A.; Girilal, M.; Mahdy, S.A.; Somsundar, S.S.; Venkatesan, R.; Kalaichelvan, P.T. Vancomycin Bound Biogenic Gold Nanoparticles: A Different Perspective for Development of Anti VRSA Agents. *Process Biochemistry* **2011**, *46*, doi:10.1016/j.procbio.2010.11.001.
21. Dalai, S.; Pakrashi, S.; Kumar, R.S.S.; Chandrasekaran, N.; Mukherjee, A. A Comparative Cytotoxicity Study of TiO₂ Nanoparticles under Light and Dark Conditions at Low Exposure Concentrations. *Toxicol Res (Camb)* **2012**, *1*, 116, doi:10.1039/c2tx00012a.
22. Selvaraj, M.; Pandurangan, P. Highly Potential Antifungal Activity of Quantum-Sized Silver Nanoparticles Against *Candida Albicans*. **2014**, doi:10.1007/s12010-014-0782-9.
23. Tängdén, T. Combination Antibiotic Therapy for Multidrug-Resistant Gram-Negative Bacteria. *Ups J Med Sci* **2014**, *119*, 149–153.
24. Paul, M.; Lador, A.; Grozinsky-Glasberg, S.; Leibovici, L. Beta Lactam Antibiotic Monotherapy versus Beta Lactam-Aminoglycoside Antibiotic Combination Therapy for Sepsis. *Cochrane Database of Systematic Reviews* **2014**, *2014*.
25. Mba, I.E.; Emeka, .; Nweze, I. Nanoparticles as Therapeutic Options for Treating Multidrug-Resistant Bacteria: Research Progress, Challenges, and Prospects. *World J Microbiol Biotechnol* **2021**, *37*, 3, doi:10.1007/s11274-021-03070-x.
26. Habeeb, H.B.; 1☉, R.; Dhandapani, R.; 1☉, I.D.; Palanivel, V.; Thangavelu, S.; Paramasivam Id, R.; Muthupandian Id, S. Bioengineered Phytomolecules-Capped Silver Nanoparticles Using *Carissa Carandas* Leaf Extract to Embed on to Urinary Catheter to Combat UTI Pathogens. **2021**, doi:10.1371/journal.pone.0256748.
27. Campo-Bele~ No, C.; Villamizar-Gallardo, R.A.; L Opez-J Acome, L.E.; Gonz Alez, E.E.; Mu~ Noz-Carranza, S.; Franco, B.; Morales-Espinosa, R.; Coria-Jimenez, R.; Franco-Cendejas, R.; Hern Andez-Dur An, M.; et al. Biologically Synthesized Silver Nanoparticles as Potent Antibacterial Effective against Multidrug-Resistant *Pseudomonas Aeruginosa*. **2022**, doi:10.1111/lam.13759.
28. Shanmugam, J.; Dhayalan, M.; Riyaz, M.; Umar, S.; Gopal, M.; Khan, M.A.; Simal-Gandara, J.; Cid-Samamed, A. Green Synthesis of Silver Nanoparticles Using *Allium Cepa* Var. *Aggregatum* Natural Extract: Antibacterial and Cytotoxic Properties. *Nanomaterials* **2022**, *12*, 1725, doi:10.3390/nano12101725.
29. Lambadi, P.R.; Sharma, T.K.; Kumar, P.; Vasnani, P.; Thalluri, S.M.; Bisht, N.; Pathania, R.; Navani, N.K. Facile Biofunctionalization of Silver Nanoparticles for Enhanced Antibacterial Properties, Endotoxin Removal, and Biofilm Control. *Int J Nanomedicine* **2015**, *10*, 2155–2171, doi:10.2147/IJN.S72923.
30. Nirmala Grace, A.; Pandian, K. Antibacterial Efficacy of Aminoglycosidic Antibiotics Protected Gold Nanoparticles-A Brief Study. *Colloids Surf A Physicochem Eng Asp* **2007**, *297*, 63–70, doi:10.1016/j.colsurfa.2006.10.024.
31. Megha Shyam, M.; Afrasim Moin, R.; Medishetti, K.R.; Raichur, A.M.; Kumar, B.R.P. Dual Drug Conjugate Loaded Nanoparticles for the Treatment of Cancer. *Curr Drug Deliv* **2015**, *12*, 782–794, doi:10.2174/1567201812666150507120452.
32. Ganeshkumar, M.; Sathishkumar, M.; Ponrasu, T.; Dinesh, M.G.; Suguna, L. Spontaneous Ultra Fast Synthesis of Gold Nanoparticles Using *Punica Granatum* for Cancer Targeted Drug Delivery. *Colloids Surf B Biointerfaces* **2013**, *106*, 208–216, doi:10.1016/j.colsurfb.2013.01.035.
33. Shruthi, T.S.; Meghana, M.R.; Medha, M.U.; Sanjana, S.; Navya, P.N.; Kumar Daima, H. Streptomycin Functionalization on Silver Nanoparticles for Improved Antibacterial Activity. *Mater Today Proc* **2019**, *10*, 8–15, doi:10.1016/J.MATPR.2019.02.181.
34. Debalina, B.; Saha, B.; Mukherjee, A.; Santra, C.R. Gold Nanoparticles Conjugated Antibiotics : Stability and Functional Evaluation. *Nanoscience and Nanotechnology* **2012**, *2*, 14–21, doi:10.5923/j.nn.20120202.04.
35. Rai, A.; Prabhune, A.; Perry, C.C. Antibiotic Mediated Synthesis of Gold Nanoparticles with Potent Antimicrobial Activity and Their Application in Antimicrobial Coatings. *J Mater Chem* **2010**, *20*, 6789–6798, doi:10.1039/c0jm00817f.
36. Renuga Devi, T.S.; Gayathri, S. FTIR And FT-Raman Spectral Analysis of Paclitaxel Drugs. *Int. J Pharm Sci Rev Res* **2010**, *2*, 106–110.
37. Woods, G.L.; Washington, J.A. Mandell, Douglas & Benett's Principles and Practice of Infectious Diseases. In *The clinician and the microbiology laboratory*; G.Mandell, J. Benett, R.D., Ed.; Churchill, Livingston, Philadelphia PA, 1995; pp. 169–199.
38. Das, B.; Dash, S.K.; Mandal, D.; Ghosh, T.; Chattopadhyay, S.; Tripathy, S.; Das, S.; Dey, S.K.; Das, D.; Roy, S. Green Synthesized Silver Nanoparticles Destroy Multidrug Resistant Bacteria via Reactive Oxygen Species Mediated Membrane Damage. *Arabian Journal of Chemistry* **2017**, *10*, 862–876, doi:10.1016/j.arabjc.2015.08.008.
39. Swathy, J.R.; Sankar, M.U.; Chaudhary, A.; Aigal, S.; Pradeep, T.; States, U.; Protection, E. Antimicrobial Silver: An Unprecedented Anion Effect. *Sci Rep* **2014**, *4*, 1–5, doi:10.1038/srep07161.

40. Dutta, T.; Chowdhury, S.K.; Ghosh, N.N.; Chattopadhyay, A.P.; Das, M.; Mandal, V. Green Synthesis of Antimicrobial Silver Nanoparticles Using Fruit Extract of *Glycosmis Pentaphylla* and Its Theoretical Explanations. *J Mol Struct* **2022**, *1247*, 131361, doi:10.1016/J.MOLSTRUC.2021.131361.
41. Eltarahony, M.; Ibrahim, A.; El-Shall, H.; Ibrahim, E.; Althobaiti, F.; Fayad, E. Molecules Antibacterial, Antifungal and Antibiofilm Activities of Silver Nanoparticles Supported by Crude Bioactive Metabolites of Bionanofactories Isolated from Lake Mariout. **2021**, doi:10.3390/molecules26103027.
42. Morones, J.R.; Elechiguerra, J.L.; Camacho, A.; Holt, K.; Kouri, J.B.; Ramírez, J.T.; Yacaman, M.J. The Bactericidal Effect of Silver Nanoparticles. *Nanotechnology* **2005**, *16*, 2346–2353, doi:10.1088/0957-4484/16/10/059.
43. AshaRani, P. V.; Mun, G.L.K.; Hande, M.P.; Valiyaveetil, S. Cytotoxicity and Genotoxicity of Silver Nanoparticles in Human Cells. *ACS Nano* **2009**, *3*, 279–290, doi:10.1021/nn800596w.
44. Barik, T.K.; Sahu, B.; Swain, V. Nanosilica - From Medicine to Pest Control. *Parasitol Res* **2008**, *103*, 253–258.
45. Lin, Y.S.; Haynes, C.L. Impacts of Mesoporous Silica Nanoparticle Size, Pore Ordering, and Pore Integrity on Hemolytic Activity. *J Am Chem Soc* **2010**, *132*, 4834–4842, doi:10.1021/ja910846q.
46. Li, S.; Zhu, R.; Zhu, H.; Xue, M.; Sun, X.; Yao, S.; Wang, S. Nanotoxicity of TiO₂ Nanoparticles to Erythrocyte in Vitro. *Food and Chemical Toxicology* **2008**, *46*, 3626–3631, doi:10.1016/j.fct.2008.09.012.
47. Kim, D.; El-Shall, H.; Dennis, D.; Morey, T. Interaction of PLGA Nanoparticles with Human Blood Constituents. *Colloids Surf B Biointerfaces* **2005**, *40*, 83–91, doi:10.1016/j.colsurfb.2004.05.007.
48. Praveen, K.-K.; Paul, W.; P-Sharma, C. Green Synthesis of Gold Nanoparticles with Zingiber Officinale Extract: Characterization and Blood Compatibility. *Process Biochemistry* **2011**, *46*, 2007–2013, doi:10.1016/j.procbio.2011.07.011.
49. Sen, I.-K.; Kumar, A.; Chakraborti, S.; Dey, B. Green Synthesis of Silver Nanoparticles Using Glucan from Mushroom and Study of Antibacterial Activity. *Int J Biol Macromol* **2013**, *62*, 439–449, doi:10.1016/j.ijbiomac.2013.09.019.
50. Shiny, P.J.; Mukherjee, A.; Chandrasekaran, N. Haemocompatibility Assessment of Synthesised Platinum Nanoparticles and Its Implication in Biology. *Bioprocess Biosyst Eng* **2014**, *37*, 991–997, doi:10.1007/s00449-013-1069-1.
51. Raja, A.; Salique, S.M.; Gajalakshmi, P.; James, A. Antibacterial and Hemolytic Activity Nanoparticles from *Catharanthus Roseus* Green. *International Journal of Pharmaceutical Sciences and Nanotechnology* **2016**, *9*, 3112–3117.
52. Srinath, B.S.; Namratha, K.; Byrappa, K. *Eco-Friendly Synthesis of Gold Nanoparticles by Gold Mine Bacteria Brevibacillus Formosus and Their Antibacterial and Biocompatible Studies*; 2017; Vol. 7.
53. Yiing Yee, F.; Periasamy, V.; Kiew, L.V.; Gnana-Kumar, G. Curcuma Mangga -Mediated Synthesis of Gold Nanoparticles : Characterization , Stability , Cytotoxicity , and Blood Compatibility. *Nanomaterials* **2017**, *7*, 1–14, doi:10.3390/nano7060123.
54. Asharani, P. v.; Sethu, S.; Vadukumpully, S.; Zhong, S.; Lim, C.T.; Hande, M.P.; Valiyaveetil, S. Investigations on the Structural Damage in Human Erythrocytes Exposed to Silver, Gold, and Platinum Nanoparticles. *Adv Funct Mater* **2010**, *20*, doi:10.1002/adfm.200901846.
55. Asharani, P. V.; Sethu, S.; Vadukumpully, S.; Zhong, S.; Lim, C.T.; Hande, M.P.; Valiyaveetil, S. Investigations on the Structural Damage in Human Erythrocytes Exposed to Silver, Gold, and Platinum Nanoparticles. *Adv Funct Mater* **2010**, *20*, 1233–1242, doi:10.1002/adfm.200901846.
56. Goodman, C.M.; McCusker, C.D.; Yilmaz, T.; Rotello, V.M. Toxicity of Gold Nanoparticles Functionalized with Cationic and Anionic Side Chains. *Bioconjug Chem* **2004**, *15*, 897–900, doi:10.1021/bc049951i.

Disclaimer/Publisher's Note: The statements, opinions and data contained in all publications are solely those of the individual author(s) and contributor(s) and not of MDPI and/or the editor(s). MDPI and/or the editor(s) disclaim responsibility for any injury to people or property resulting from any ideas, methods, instructions or products referred to in the content.